Title

Effect of Surface–Molecule Interactions on Molecular Loading Capacity of Nanoporous Gold Thin Films

Journal

The Journal of Physical Chemistry C, 120(34)

ISSN

1932-7447

Authors

Polat, Ozge

Seker, Erkin

Publication Date

2016-09-01

DOI

10.1021/acs.jpcc.6b05802

Peer reviewed

THE JOURNAL OF PHYSICAL CHEMISTRY C

Article

Effect of Surface-Molecule Interactions on Molecular Loading Capacity of Nanoporous Gold Thin Films

Ozge Polat, and Erkin Seker

J. Phys. Chem. C, **Just Accepted Manuscript** • Publication Date (Web): 10 Aug 2016

ACS Publications

The Journal of Physical Chemistry C is published by the American Chemical Society. 1155 Sixteenth Street N.W., Washington, DC 20036

Effect of Surface-Molecule Interactions on Molecular Loading Capacity of Nanoporous Gold Thin Films

Ozge Polat[a], Erkin Seker[b*]

[a] Department of Chemical Engineering and Materials Science

[b] Department of Electrical and Computer Engineering

University of California Davis, Davis, California 95616, USA

*Corresponding Author:

e-mail:eseker@ucdavis.edu,

Phone: (530) 752-7300

ABSTRACT

Surface-molecule interactions play an essential role in loading capacity and release kinetics in nanostructured materials with high surface area-to-volume ratio. Engineering the surfaces via immobilizing functional moieties is therefore a versatile means to enhance the performance of drug delivery platforms with nanostructured components. Nanoporous gold (np-Au), with its high effective surface area, well established gold-thiol chemistry, and tunable pore morphology, is an emerging material not only for drug delivery applications but also as a model system to study the influence of physicochemical surface properties on molecular loading capacity and release kinetics. Here, we functionalize np-Au with self-assembled monolayers (SAMs) of alkanethiols with varying functional groups and chain lengths, and use fluorescein (a small-molecule drug surrogate) to provide insight into the relationship between surface properties and molecular release. The results revealed that electrostatic interactions dominate the loading capacity for short SAMs (two carbons). As SAM length increases the loading capacity displays a non-monotonic dependence on chain length, where for medium-length SAMs (six carbons) allow for higher loading plausibly due to denser SAM surface packing. For longer SAMs (11 carbons), the steric hindrance due to long chains crowds the pores, thereby hampering fluorescein access to the deeper pore layers, consequently reducing loading capacity.

INTRODUCTION

A common goal for most drug delivery platforms is to maintain the delivered dose within a specific therapeutic window during therapy duration. For these platforms, high drug loading capacity and tunable release kinetics are two important figures of merit[1]. Nanostructured materials have shown significant promise in achieving these requirements, where carbon nanotubes, nanoporous anodic alumina, nanotubular titania, and porous silicon are often used[2-5]. For these material systems with high effective surface area, surface-drug molecule interactions play an essential role in loading capacity and release kinetics[6-7]. Properties of the drug molecules (e.g., electrical charge, size, chemical reactivity), the materials (e.g., morphology, surface charge), and the liquid medium where the molecules are delivered (e.g., ionic strength, pH) are all crucial factors in dictating drug delivery performance[2, 6] . Nanoporous gold (np-Au), with its high effective surface area, well established gold-thiol-mediated surface modifications, and tunable pore morphology, is a promising material for drug delivery applications and studying the influence of physicochemical surface properties on the molecule-loading capacity and release kinetics[8-15]. Our previous studies have focused on the effect of pore morphology and elution medium constituents on the molecular release from np-Au coatings[11, 16]. These studies highlighted the significance of surface-molecule interactions in dictating molecular release from np-Au. The goal of this paper is to leverage the importance of surface-molecule interactions and systematically modify np-Au surfaces with SAMs of alkanethiols with varying electrical charge and monolayer thickness on the surface in order to provide insight into the relationship between surface properties and molecular release.

MATERIALS AND METHODS

Materials and Chemicals Reagents

Glass coverslips (12 mm x 24 mm), which are used as substrates for np-Au thin films, were purchased from Electron Microscopy Sciences. Kurt J. Lesker sputtering targets (chrome, gold, silver) were used for depositing gold-silver alloys (precursor to np-Au). Polydimethylsiloxane (PDMS) elastomer sheets were purchased from B & J Rubber Products and used as stencil masks to produce np-Au patterns on glass coverslips. Fluorescein sodium salt, sodium hydroxide, nitric acid (70%), 6-mercapto-1-hexanol, 6-mercaptohexanoic acid, 6-amino-1-hexanethiol hydrochloride, calcium chloride, calcium nitrate monohydrate, and 200-proof molecular biology grade ethanol were all purchased from Sigma-Aldrich. 11-amino-1-undecanethiol hydrochloride was purchased from Dojindo. Dulbecco`s phosphate-buffered saline without calcium and magnesium (1x-PBS) was purchased from Life Technologies.

Fabrication and Characterization of np-Au Release Samples

Our previous work describes the detailed fabrication of patterned np-Au thin films used in the release experiments[11, 16]. Briefly, in order to fabricate the *release chips* (also referred to as *release samples*) used for molecular release from 3 mm x 3 mm np-Au patterns, we sputtered a stack of metal layers through a laser-cut PDMS stencil mask temporarily placed on glass coverslips. The stack of deposited materials consisted of chrome adhesion layer (160 nm), gold seed layer (80 nm), and gold-silver alloy layer (600 nm) obtained by co-sputtering gold and silver. The final metal films were immersed in 70% nitric acid at 55 °C for 15 minutes to dealloy the gold-silver layer to produce the release chips. Scanning electron microscopy (SEM, FEI Nova NanoSEM430) was used to determine the thickness and morphological features of the np-Au films. The silver and gold composition of the films were determined by energy dispersive X-ray spectroscopy (EDS, Oxford Inca Energy). The SEM images were analyzed with a

combination of ImageJ segmentation methods and a custom MatLab script to extract pore and ligament sizes.

Surface Modification and Contact Angle Measurements

The np-Au release chips were cleaned with oxygen plasma at 10 W for 1 minute in order to increase the hydrophilicity of the surface before any experimental procedure. Thiol solutions (4 mM) were prepared in molecular biology grade ethanol. The release chips were immersed in these solutions immediately following the plasma treatment and incubated for 24 hours. After incubation, the samples were rinsed with ethanol and dried. Contact angles of np-Au films modified with different functional SAMs were determined with a goniometer and calculated by Drop Analysis plug-in of ImageJ[17].

Loading and Molecular Release Quantification

The SAM-modified np-Au chips were incubated overnight in 250 µl-microcentrifuge tubes filled with *loading medium* (10 mM fluorescein sodium salt in deionized (DI) water, where a steady-state loading isotherm is typically reached for bare np-Au surfaces) at room temperature[11]. The loading medium was then aspirated and the samples were rinsed with DI water to remove residual fluorescein from the outer surfaces of the samples. After the rinse, each chip was placed into a new microcentrifuge tube filled with *release medium* of interest (DI water or PBS) to initiate fluorescein release from the np-Au chips. At successive time points, 10 µL of solution was sampled from the elution tube (following pipet agitation to ensure homogeneity) and mixed with 10 µL of 50 mM NaOH to enhance fluorescence intensity[11, 16]. The fluorescence intensity of the resulting solution was quantified with NanoDrop 3300 fluorospectrometer at a peak emission wavelength of 515 nm. The fluorescence measurements were converted to corresponding concentration and mass of released fluorescein via calibration curves. Once the release profile reached a steady-state, last three data points on the plateau were averaged and divided by the

footprint of the patterned film to calculate the loading capacity. Data points and error bars in the figures are averages and standard errors of measurements from at least five different release chips.

RESULTS AND DISCUSSION

The central aim of this study was to investigate the effect of surface-molecule interactions on the loading capacity of fluorescein by modifying np-Au surfaces (Figure 1) with alkanethiols of different functional groups and chain lengths. The samples used in this study were fabricated by dealloying the sputter-deposited precursor gold-silver alloy. The elemental composition of the films before and after dealloying were respectively 30%:70% (Au:Ag, atomic percent) and 3-5% of residual silver. The resulting porous films had a distribution of pores[18], where average ligament (light gray areas) and pore (small dark areas) width were 144 ± 12 nm and 78 ± 7 nm respectively. Tensile stress accumulation during the dealloying step results in hairline cracks (large connected darker regions in top SEM view) throughout the film, which were included in the determination of pore width[19]. The influence of cracks on loading capacity and release kinetics have been reported previously[11].

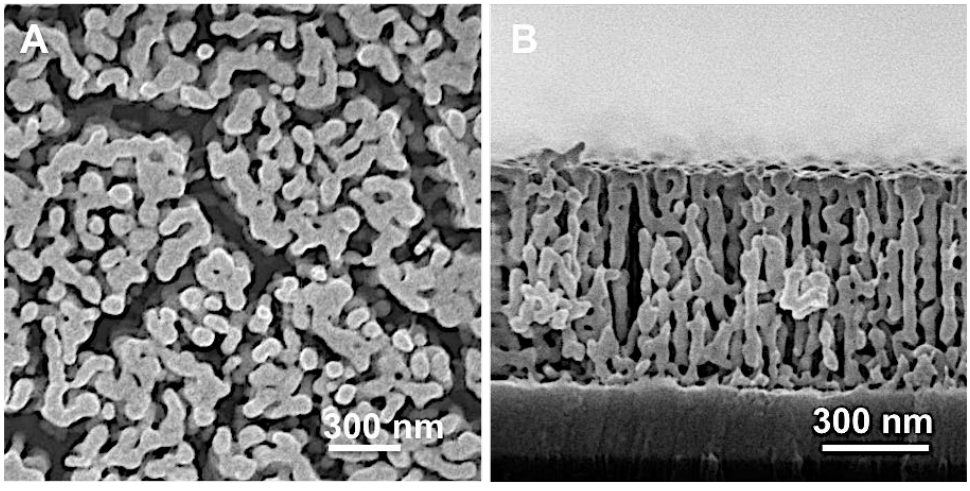

Figure 1. (A) Top- and (B) cross-sectional scanning electron micrographs of non-modified np-Au thin films used in the experiments.

Effect of Functional Group on Loading Capacity

The use of different functional end-groups on thiolated surfaces allows for a systematic study of surface charge and resulting surface-molecule interactions. To that end, we immobilized moieties with distinct electrical charges on the np-Au surface via anchoring thiols with different functional groups. More specifically, the np-Au surfaces were separately modified with 6-mercapto-1-hexanol (6-OH), 6-amino-1-hexanethiol (6-NH_2), and 6-mercaptohexanoicacid (6-COOH). Isoelectric points of amine- and carboxylic acid-terminated SAMs on planar gold surfaces are reported as 6.5 and 3.5 respectively[20]. The pH of DI water and PBS used in the current experiments were 6.5 ± 0.1 and 7.4 ± 0.1 respectively, thereby, rendering amine-modified np-Au positively-charged and carboxyl-modified np-Au negatively-charged. On the other hand, the alcohol-modified np-Au did not have a net electrical charge. The fluorescein molecules acquire a negative charge in the solutions used. In order to ensure that the surface modification does not lead to hydrophobic surfaces and allows for loading and release medium to permeate the porous structure, we performed contact angle measurements on each modified surface. The average contact angle for all surfaces modification was 32.4° ± 10.9°, indicating a highly hydrophilic surface. The neutral (6-OH) and negatively-charged (6-COOH) np-Au films released only a small amount of fluorescein compared to the positively-charged (6-NH_2) or the non-modified np-Au films, consequently leading to drastic differences in loading capacity as a function of surface functionalization (Figure 2).

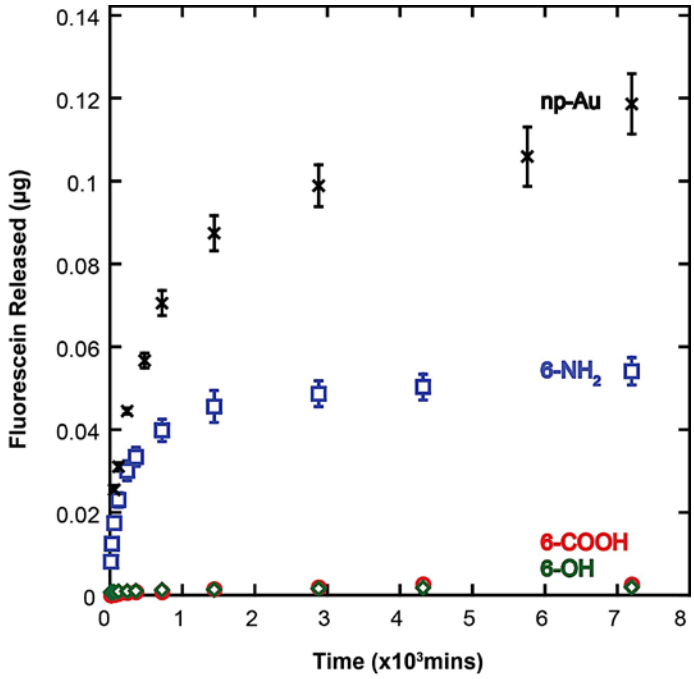

Figure 2. Fluorescein release from non-modified np-Au, 6-NH_2, 6-COOH, and 6-OH modified np-Au thin films. The functional end-group affects the loaded fluorescein amount via the interactions between fluorescein and the surface group.

As expected, the carboxyl-modified surfaces led to minimal loading due to the strong electrostatic repulsion between the negatively-charged carboxylic acid groups and the negatively-charged fluorescein molecules. Via the similar electrostatic interaction based mechanism, the amine-modified np-Au displayed high loading capacity (0.6 µg/cm^2) due to the positively-charged surface, indicating that the loading capacity can be drastically changed by controlling the surface-molecule interactions by tailoring surface properties via SAM immobilization. The loading capacity for the amine-modified np-Au was approximately two-fold less than non-modified np-Au, which can be attributed to the reduction in the number of sites available for fluorescein adsorption for the SAM case (amine groups separated due to electrostatic repulsion[21]) in comparison to non-modified gold (densely packed gold lattice)[16]. The packing density of fluorescein on bare np-Au can be estimated as 10.7 molecules/nm^2 based on hexagonal packing monolayer coverage assuming fluorescein hydrodynamic radius of 0.58 nm

(calculated by Stokes-Einstein equation)[11]. On the other hand, packing density of alkanethiolates with comparable size and charge (consequently the functional group density for fluorescein adsorption) on Au (111) is approximately 5 molecules/nm^2 based on theoretical calculations[22]. This two-fold decrease in adsorption site density is consistent with the similar decrease in loading capacity for amine-modified np-Au compared to the bare np-Au.

The loading capacity for electrically-neutral OH-modified np-Au surface was negligible even though the bare np-Au also does not present a prominent surface charge. In addition to the difference in density of adsorption sites on the two surfaces for fluorescein loading, we also attribute this to gold atoms being more polarizable than the hydroxyl groups, thereby procuring a larger induced dipole than the hydroxyl group[23]. Briefly, the interactions between fluorescein and gold are ion-induced dipole, while the interactions between fluorescein and hydroxyl groups are ion-dipole. The energy of interaction between an ion and dipole scales with r^{-2}, while for an ion-induced dipole the scaling is r^{-4}, where r is the distance between the point charge and the dipole or induced dipole[24]. If approximated that during loading (i.e., adsorption of fluorescein molecules onto the surface) r approaches to zero, the interaction energy would be higher for the case of ion-induced dipole (fluorescein and non-modified np-Au interaction) and lead to a higher loading capacity than that for hydroxyl-modified np-Au.

In order to further test the effect of the electrostatic interactions on loading capacity, we introduced cations into the loading medium by supplementing the fluorescein solution with calcium salts. Binding of divalent metal ions such as calcium onto SAM-modified electrode surfaces is well known[25]. Here, we test the hypothesis that calcium cations in the loading medium would improve loading capacity by acting as electrostatic linkages between negatively-charged fluorescein molecules and the negatively-charged carboxyl-treated np-Au. To that end, we used 100 mM $CaCl_2$ as the loading medium and PBS was selected as the elution medium. It

should be noted that halide ions results in a fast release of fluorescein from non-modified np-Au films by substituting adsorbed fluorescein molecules due to high gold-halide affinity[16]. In order to control the possible influence of chloride in this experiment and to decouple calcium ions' effect on loading capacity, 100 mM $Ca(NO_3)_2$ was used for the loading medium as a control group. When modified surfaces were incubated in fluorescein solutions prepared in $CaCl_2$ and $Ca(NO_3)_2$, a higher loading capacity (0.24 and 0.25 μg/cm^2) was observed compared to that seen for samples incubated in fluorescein solution without the calcium cation linkers (Figure 3).

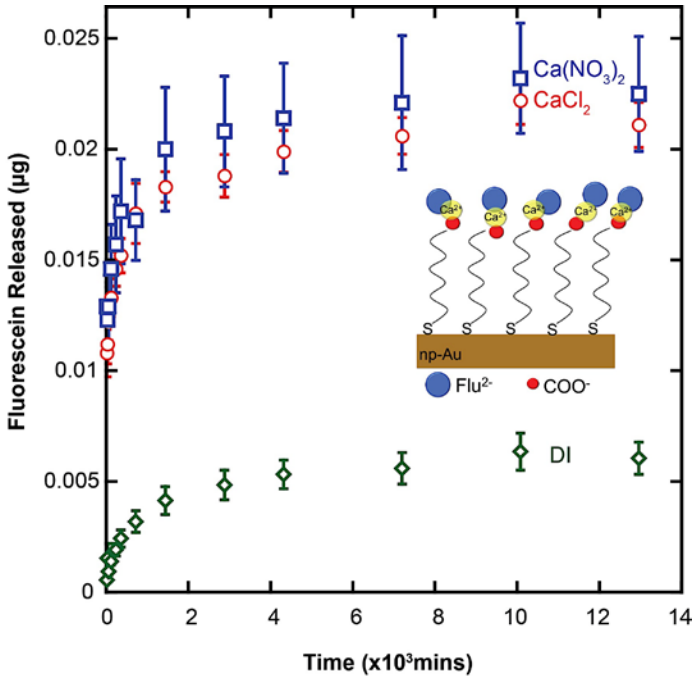

Figure 3. Release into PBS from carboxyl-modified np-Au films incubated in fluorescein solution prepared in only DI water, 100 mM $CaCl_2$, and 100 mM $Ca(NO_3)_2$.

There was not a significant difference between loading capacities of the chips loaded in $CaCl_2$ and $Ca(NO_3)_2$ suggesting that the presence of halide did not influence the fluorescein release since SAM makes gold surface inaccessible in both of the cases. This insensitivity to the halide also indicates that np-Au surface must be largely covered by the SAM, confirming the effectiveness of the thiol-based SAM formation on gold.

Effect of Chain Length on Loading Capacity and Release Kinetics

The packing density of alkanethiols is known to increase with increasing hydrocarbon chain length due to increased Van der Waals interactions between alkyl chains[26]. This suggests that with increasing chain length, that is, high density SAM, the loading capacity should increase due to increased positive charge on the surface. However, for materials composed of interconnected nano-channels (such as np-Au), the increasing chain length may also lead to steric effects and hinder the transport of molecules through the porous network. In order to study these two competing hypothesized effects of SAM chain length on loading capacity, we contrasted cysteamine (2-NH_2), 6-NH_2, and 11-amino-1-undecanethiol (11-NH_2) for modifying the np-Au films. We specifically chose the amine-based modification since among the other functional alkanethiols tested; the amine-modification resulted in the higher loading capacity. The loading capacity displayed a non-monotonic dependence on chain-length, where for medium-length SAMs (six carbons) resulted in the highest loading capacity while the short and long SAMs exhibited less loading (Figure 4A). Fluorescein release into PBS (in comparison to deionized water) was faster for both the amine-modified and bare np-Au surfaces (Figure 4B).

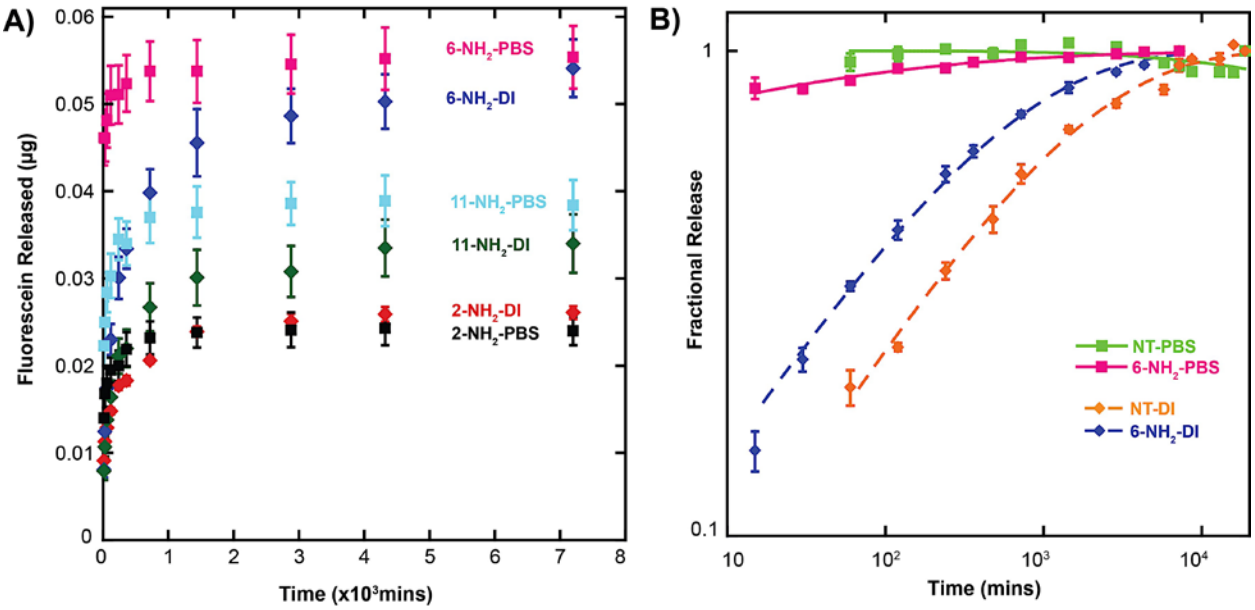

Figure 4. (A) Release from 2-NH_2, 6-NH_2, and 11-NH_2 modified np-Au films into DI water and PBS. (B) The corresponding fractional release profiles into DI water and PBS for the three different surface modifications.

As stated earlier, the packing density of SAMs increases with chain length[26], thereby a monotonic increase in loading capacity is expected for np-Au surfaces modified with amino-thiol SAMs of increasing chain length. However, as the packing density increases, the alkanethiols become more brush-like and extend further away from the surface. Even though the longest chain tested here would have a length of 1.6 nm[27], this may still lead to considerable hindrance in transport at sites where channels narrow down to a few nanometers (Figure 1B), as confirmed by pore size distributions reported previously[18]. It is probable that for a bicontinuous nanochannel network that constitutes np-Au, even a small number of constrictions along a channel may hinder the access to the deeper pores (plausibly via steric crowding and/or increased probability of fluorescein-surface adsorption/desorption events), thereby reducing loading capacity. Taken together, the observed *non-monotonic* trend of loading capacity for a SAM-modified nanostructured material can be attributed to the interplay of two mechanisms: (i) chain-length dependent packing density and (ii) steric hindrance-driven surface accessibility. The results suggest that even though more fluorescein molecules can be adsorbed onto the amine-modified surfaces with increasing chain length (Figure 5A), the increasing steric hindrance to molecular permeation limits the available np-Au surface that can be loaded by fluorescein (Figure 5B). The combination of the two mechanisms was deemed responsible for the observed non-monotonic trend.

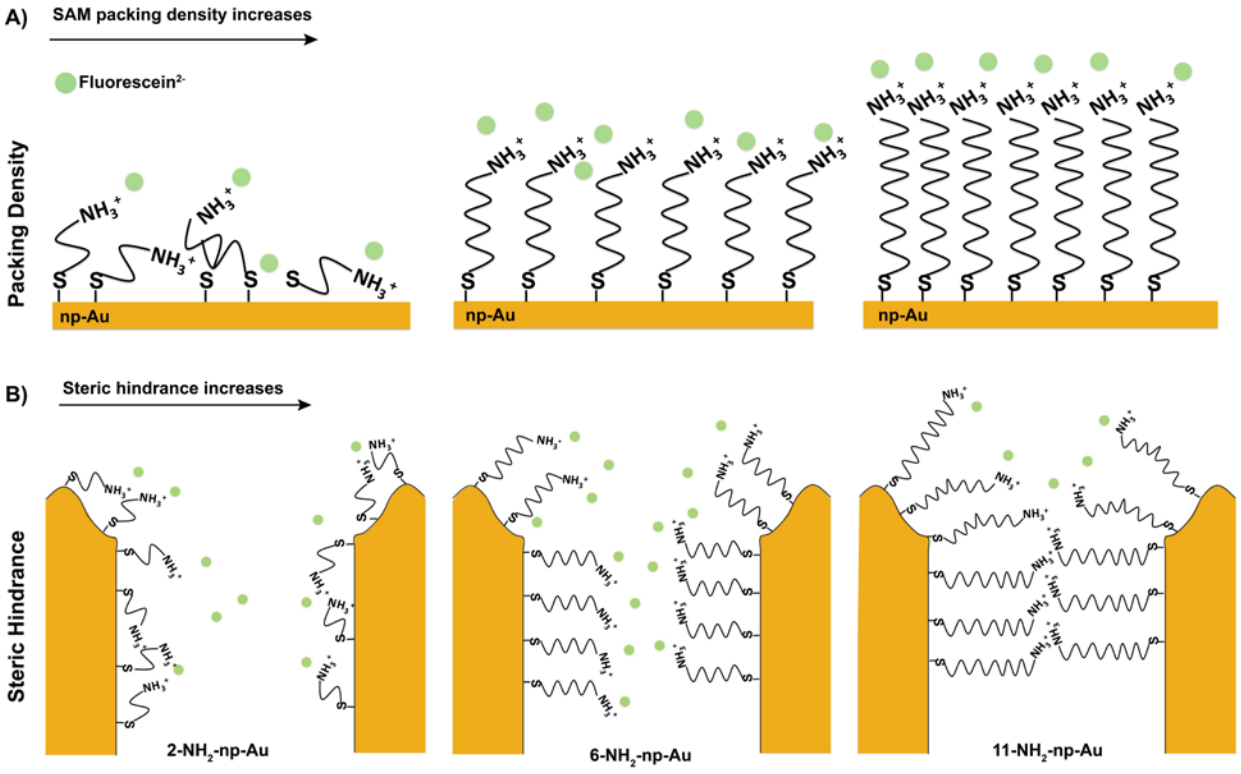

Figure 5. Schematic illustration of loading and transport of molecules for SAM-modified surfaces. (A) SAM density, thus loading capacity, increases for surface modification with increasing chain length. (B) Steric hindrance due to thicker SAM layer for longer alkanethiols limits molecule permeation to deeper surfaces. Pore and molecule sizes are exaggerated for clarity.

As seen in Figure 4A, the release into PBS suggests a similar loading capacity compared to that for release into DI water; however, a faster release is observed for the PBS case (Figure 4B). This is consistent with our previous results that indicated fast release of fluorescein from non-modified np-Au films in PBS due to rapid displacement of surface-bound fluorescein molecules by chloride ions in PBS with high affinity to gold. A similar, yet less pronounced behavior is evident for the amine-modified np-Au films (Figure 4B). Since shown earlier, non-modified gold surface is largely screened by the SAM layer, therefore halide-gold interaction is not likely. However, chloride anions can electrostatically interact with the positively-charged amine functional groups, thereby disrupting the fluorescein-amine complexes. Unlike the halide-bare

gold case, where the interaction is thermodynamically-driven, we expect the fluorescein-amine-chloride interaction to be kinetically-driven, thereby the release profile being less sensitive to the presence of halides. It should be noted that the molecular release in np-Au is composed of desorption of surface-bound molecules and their efflux through the porous network. Since both of these processes depend strongly on the SAM packing density and extent of steric hindrance, it is difficult to make definitive conclusions with regards to the effect of SAMs on release kinetics.

CONCLUSION

We used np-Au as a model nanostructured material for studying molecular loading and release, and demonstrated the effect of surface modification with functional alkanethiols on molecular release behavior. The results revealed that electrostatic interactions dominated the loading capacity for np-Au films with different functional groups while packing density and steric effects played a role in determining loading capacity of np-Au films modified with different chain length of amine-terminated alkanethiols. Increase in the loading capacity displayed a non-monotonic dependence on chain-length, where for medium-length SAMs (six carbons) allowed for higher loading compared to short-length (two carbons) due to denser SAM surface packing. For longer SAMs (eleven carbons), the steric hindrance due to long chains crowded the pores, thereby hampering fluorescein access to deeper pore layers and consequently reducing loading capacity. The approach described here can be expanded to use of other alkanethiols with different functional groups to modulate the surface-molecule interactions for custom cases such as release in specific pH conditions[28-29]. We expect that this work will assist in development of novel drug delivery platforms based on nanostructured materials.

AUTHOR INFORMATION

Corresponding Author

*E-mail: eseker@ucdavis.edu; Tel: (530) 752-7300

Notes:

The authors declare no competing financial interest.

ACKNOWLEDGMENT

We gratefully acknowledge the support from UC Lab Fees Research Program Award (12-LR-237197), UC Davis Research Investments in the Sciences & Engineering (RISE) Award, and National Science Foundation Awards (CBET-1512745 and CBET&DMR-1454426). We also thank Dr. Patricia Losada Pérez (University of Hasselt, Belgium) and Dr. Zimple Matharu (UC Davis) for discussions on thiol-surface-fluorescein interactions, and Prof. Tingrui Pan (UC Davis) for his help in stencil mask preparation.

REFERENCES

1. Goldberg, M.; Langer, R.; Jia, X., Nanostructured Materials for Applications in Drug Delivery and Tissue Engineering. *J. of Biomater. Sci. Polym. Ed.* **2007**, *18*, 241-268.

2. Gultepe, E.; Nagesha, D.; Sridhar, S.; Amiji, M., Nanoporous Inorganic Membranes or Coatings for Sustained Drug Delivery in Implantable Devices. *Adv. Drug Del. Rev.* **2010**, *62*, 305-315.

3. Losic, D.; Simovic, S., Self-Ordered Nanopore and Nanotube Platforms for Drug Delivery Applications. *Expert Opin. Drug Deliv.* **2009**, *6*, 1363-1381.

4. Arruebo, M., Drug Delivery from Structured Porous Inorganic Materials. *Wiley Interdiscip. Rev. Nanomed Nanobiotechnol.* **2012**, *4*, 16-30.

5. Tran, P. A.; Zhang, L.; Webster, T. J., Carbon Nanofibers and Carbon Nanotubes in Regenerative Medicine. *Adv. Drug Deliv. Rev.* **2009**, *61*, 1097-1114.

6. Aw, M. S.; Kurian, M.; Losic, D., Non-Eroding Drug-Releasing Implants with Ordered Nanoporous and Nanotubular Structures: Concepts for Controlling Drug Release. *Biomater. Sci.* **2014**, *2*, 10-34.

7. Vallet-Regí, M.; Balas, F.; Arcos, D., Mesoporous Materials for Drug Delivery. *Angew. Chem. Int. Ed.* **2007**, *46*, 7548-7558.

8. Seker, E.; Berdichevsky, Y.; Staley, K. J.; Yarmush, M. L., Microfabrication-Compatible Nanoporous Gold Foams as Biomaterials for Drug Delivery. *Adv. Healthc. Mater.* **2012**, *1*, 172-6.

9. Santos, G. M.; Zhao, F.; Zeng, J.; Shih, W.-C., Characterization of Nanoporous Gold Disks for Photothermal Light Harvesting and Light-Gated Molecular Release. *Nanoscale* **2014**, *6*, 5718-5724.

10. Garcia-Gradilla, V.; Sattayasamitsathit, S.; Soto, F.; Kuralay, F.; Yardımcı, C.; Wiitala, D.; Galarnyk, M.; Wang, J., Ultrasound-Propelled Nanoporous Gold Wire for Efficient Drug Loading and Release. *Small* **2014**, *10*, 4154-4159.

11. Kurtulus, O.; Daggumati, P.; Seker, E., Molecular Release from Patterned Nanoporous Gold Thin Films. *Nanoscale* **2014**, *6*, 7062-7071.

12. Daggumati, P.; Appelt, S.; Matharu, Z.; Marco, M. L.; Seker, E. Sequence-Specific Electrical Purification of Nucleic Acids with Nanoporous Gold Electrodes. *J. Am. Chem. Soc.* **2016**, 138 (24), 7711-7717.

13. Gittard, S. D.; Pierson, B. E.; Ha, C. M.; Wu, C. A. M.; Narayan, R. J.; Robinson, D. B., Supercapacitive Transport of Pharmacologic Agents Using Nanoporous Gold Electrodes. *Biotechnol. J* **. 2010**, *5*, 192-200.

14. Tan, Y. H.; Fujikawa, K.; Pornsuriyasak, P.; Alla, A. J.; Ganesh, N. V.; Demchenko, A. V.; Stine, K. J., Lectin–Carbohydrate Interactions on Nanoporous Gold Monoliths. *New J. Chem.* **2013**, *37*, 2150-2165.

15. McCurry, D. A.; Bailey, R. C., Nanoporous Gold Membranes as Robust Constructs for Selectively Tunable Chemical Transport. *J. Phys. Chem. C* **2016**, DOI: 10.1021/acs.jpcc.6b02759.

16. Polat, O.; Seker, E., Halide-Gated Molecular Release from Nanoporous Gold Thin Films. *J. Phys. Chem. C* **2015**, *119*, 24812-24818.

17. Stalder, A. F.; Melchior, T.; Müller, M.; Sage, D.; Blu, T.; Unser, M., Low-Bond Axisymmetric Drop Shape Analysis for Surface Tension and Contact Angle Measurements of Sessile Drops. *Colloids Surf. A Physicochem. Eng. Asp.* **2010**, *364*, 72-81.

18. Chapman, C. A.; Wang, L.; Biener, J.; Seker, E.; Biener, M. M.; Matthews, M. J., Engineering on-Chip Nanoporous Gold Material Libraries Via Precision Photothermal Treatment. *Nanoscale* **2016**, *8*, 785-795.

19. Chapman, C. A.; Daggumati, P.; Gott, S. C.; Rao, M. P.; Seker, E., Substrate Topography Guides Pore Morphology Evolution in Nanoporous Gold Thin Films. *Scripta Mater.* **2016**, *110*, 33-36.

20. Lin, W.-C.; Lee, S.-H.; Karakachian, M.; Yu, B.-Y.; Chen, Y.-Y.; Lin, Y.-C.; Kuo, C.-H.; Shyue, J.-J., Tuning the Surface Potential of Gold Substrates Arbitrarily with Self-Assembled Monolayers with Mixed Functional Groups. *Phys. Chem. Chem. Phys.* **2009**, *11*, 6199-6204.

21. Marmisollé, W. A.; Capdevila, D. A.; de la Llave, E.; Williams, F. J.; Murgida, D. H., Self-Assembled Monolayers of Nh2-Terminated Thiolates: Order, P K a, and Specific Adsorption. *Langmuir* **2013**, *29*, 5351-5359.

22. Hinterwirth, H.; Kappel, S.; Waitz, T.; Prohaska, T.; Lindner, W.; Lämmerhofer, M., Quantifying Thiol Ligand Density of Self-Assembled Monolayers on Gold Nanoparticles by Inductively Coupled Plasma–Mass Spectrometry. *ACS Nano* **2013**, *7*, 1129-1136.

23. Haynes, W. M., *Handbook of Chemistry and Physics*; CRC Press: Florida, US, 2016.

24. Butt, H.-J.; Graf, K.; Kappl, M., *Physics and Chemistry of Interfaces*; Wiley-VCH: Weinheim, Germany, 2006.

25. Burshtain, D.; Mandler, D., The Effect of Surface Attachment on Ligand Binding: Studying the Association of Mg 2+, Ca 2+ and Sr 2+ by 1-Thioglycerol and 1, 4-Dithiothreitol Monolayers. *Phys. Chem. Chem. Phys.* **2006**, *8*, 158-164.

26. Vericat, C.; Vela, M.; Benitez, G.; Carro, P.; Salvarezza, R., Self-Assembled Monolayers of Thiols and Dithiols on Gold: New Challenges for a Well-Known System. *Chem. Soc. Rev.* **2010**, *39*, 1805-1834.

27. Campiña, J. M.; Martins, A.; Silva, F., Selective Permeation of a Liquidlike Self-Assembled Monolayer of 11-Amino-1-Undecanethiol on Polycrystalline Gold by Highly Charged Electroactive Probes. *J. Phys. Chem. C* **2007**, *111*, 5351-5362.

28. Moerz, S. T.; Huber, P., Ph-Dependent Selective Protein Adsorption into Mesoporous Silica. *J. Phys. Chem. C* **2015**, *119*, 27072-27079.

29. Buchsbaum, S. F.; Nguyen, G.; Howorka, S.; Siwy, Z. S., DNA-Modified Polymer Pores Allow Ph-and Voltage-Gated Control of Channel Flux. *J. Am. Chem. Soc.* **2014**, *136*, 9902-9905.

TABLE OF CONTENTS IMAGE